Design of an adaptive Fuzzy control system for dual star induction motor drives

Article *in* Advances in Electrical and Computer Engineering · August 2018

CITATIONS
2

READS
200

5 authors, including:

Luis Guasch-Pesquer
Universitat Rovira i Virgili
51 PUBLICATIONS **333** CITATIONS
SEE PROFILE

Lamia Youb
University of Batna 2
11 PUBLICATIONS **53** CITATIONS
SEE PROFILE

Sebti Belkacem
University of Batna 2
50 PUBLICATIONS **151** CITATIONS
SEE PROFILE

Farid Naceri
university of Batna 2
12 PUBLICATIONS **82** CITATIONS
SEE PROFILE

Design of an Adaptive Fuzzy Control System for Dual Star Induction Motor Drives

Lamia YOUB[1], Sebti BELKACEM[1], Farid NACERI[1], Mihai CERNAT[2], Luis Guasch PESQUER[3]
[1]*University of Batna 2, Batna, Algeria, youblamia@yahoo.fr*
[2]*Transilvania University of Brasov, Brasov, Romania, m.cernat@unitbv.ro*
[3]*University Rovira i Virgili, Tarragona, Spain, luis.guasch@urv.cat*

***Abstract*—In this paper, a new control strategy is developed; an adaptive fuzzy controller based on Lyapunov's stability theory (AFLC) recalculates the real-time PI-fuzzy gains and combines the advantages of two robust techniques i.e. the fuzzy logic control and the adaptive one. For the new adaptive fuzzy control, we followed two steps: in the first one, a PI-fuzzy controller is designed, in the second step, the gains of a fuzzy regulator are determined. Extensive simulation results are presented to validate the proposed technique. The system is tested at different speeds and a very satisfactory performance has been achieved**.

***Index Terms*—adaptive control, fuzzy control, Lyapunov method, dual star induction motor.**

I. INTRODUCTION

The use of the dual star induction motor (DSIM), especially for high-power applications, has largely replaced asynchronous machines, whose role were predominant in the industry [1–8]. The dual star induction motor is constituted of two windings whith a phase displacement of 30 electrical degrees. These windings are usually powered by a six-phase inverter fed at variable speed. The main advantages of the DSIM are their higher torque density, higher efficiency, reduced harmonic content of the DC link current [9].

In [1-10], a model of the dual star induction motor is developed. The associated vector control is based on the decomposition of the 6-dimensional space in three orthogonal spaces. The authors deduced that the torque of the double star asynchronous machine is produced only by the flux/current interactions in a plane, conventionally called (d, q) as in the case of three-phase machines. However the control of DSIM is complicated because is is difficult to decouple the torque from the flux. To surmount these difficulty, high-performance algorithms have been developed [10-18].

In [11], the Popov stability criterion is used and the sufficient stability condition for control loops having a non-linear element was found. In fact, this amounts to find a linear characteristic that approximates the non-linear one of the mono-input regulator. In the case of a two-input regulator, the fuzzy controller is assimilated to a conventional PI-controller.

In [12-14], the authors present a sliding-mode control algorithm of a DSIM, the control ensures a good tracking performance, a fast dynamics and a short response time. However, the control law presents some disadvantages which can be summarized in two points. The first one consists of the need to have a precise information about the evolution of the system in the state space. The second disadvantage lies in the tracking phenomenon when a load torque is applied; it is possible to have a static error in the speed response, chattering phenomenon, which consists of sudden and rapid variations of the control signal, may occur.

The fuzzy logic has been a real success not only in the modelling but also in the control of double star asynchronous machines. An application using fuzzy systems has been developed in [13-19].

The Self-Tuning mechanism for induction motor has been introduced in order to tune the fuzzy parameters online in case when any disturbances occurred [20-22].

In [30-35], the authors suggested an automatic adaptation of the fuzzy rules that guarantees the stability of the control.

The present paper proposes a new control strategy based on the Lyapunov stability theory and the corresponding adaptive fuzzy controller that combines the advantages of two robust techniques, i.e. the fuzzy logic control and the adaptive control.

The remaining part of this paper is structured as follows: in Section II the mathematical model of the DSIM is presented. In Section III a vector control of the DSIM is introduced. A PI-Fuzzy control of the DSIM is proposed in Section IV. The simulation results and their discussion are presented in Section V. Finally, conclusions and future work were presented in Section VI.

II. MATHEMATICAL MODEL OF DSIM

By applying the Park transformation to the three-phase model of the DSIM (Fig. 1), we obtain the following equation system, expressed in the (d, q) reference frame [9]:

$$\begin{aligned} V_{ds1,2} &= R_{ds1,2} i_{ds1,2} + \frac{\mathrm{d}\varphi_{ds1,2}}{\mathrm{d}t} - \omega_s \varphi_{qs1,2} \\ V_{qs1,2} &= R_{qs1,2} i_{qs1,2} + \frac{\mathrm{d}\varphi_{qs1,2}}{\mathrm{d}t} + \omega_s \varphi_{ds1,2} \\ V_{dr} &= 0 = R_r i_{dr} + \frac{\mathrm{d}\varphi_{dr}}{\mathrm{d}t} - (\omega_s - \omega_r)\varphi_{qr} \\ V_{qr} &= 0 = R_r i_{qr} + \frac{\mathrm{d}\varphi_{qr}}{\mathrm{d}t} + (\omega_s - \omega_r)\varphi_{dr} \end{aligned} \quad (1)$$

The stator and rotor fluxes are expressed, respectively, by:

Digital Object Identifier 10.4316/AECE.2018.03006

$$\begin{aligned}
\varphi_{ds1,2} &= L_{s1,2} i_{ds1,2} + L_m \left(i_{ds1} + i_{ds2} + i_{dr}\right) \\
\varphi_{qs1,2} &= L_{s1,2} i_{qs1,2} + L_m \left(i_{qs1} + i_{qs2} + i_{qr}\right) \\
\varphi_{dr} &= L_r i_{dr} + L_m \left(i_{ds1} + i_{ds2} + i_{dr}\right) \\
\varphi_{qr} &= L_r i_{qr} + L_m \left(i_{qs1} + i_{qs2} + i_{qr}\right)
\end{aligned} \tag{2}$$

The model is completed by the mechanical equation:

$$J \frac{\mathrm{d}\Omega}{\mathrm{d}t} = T_e - T_r - f_r \, \Omega \tag{3}$$

where the following notations have been used:

J - inertia;
f_r - friction coefficient;
T_e - electromagnetic torque;
T_r - load torque;
Ω - mechanical speed of the rotor.

The expression of the electromagnetic torque T_e is [2]:

$$T_e = p \frac{L_m}{L_m + L_r} \left(\varphi_{dr} \left(i_{qs1} + i_{qs2}\right) - \varphi_{qr} \left(i_{ds1} + i_{ds2}\right)\right) \tag{4}$$

where p is the number of pole pairs.

Fig. 1 shows the schematic representation of the stator and rotor windings of the DSIM.

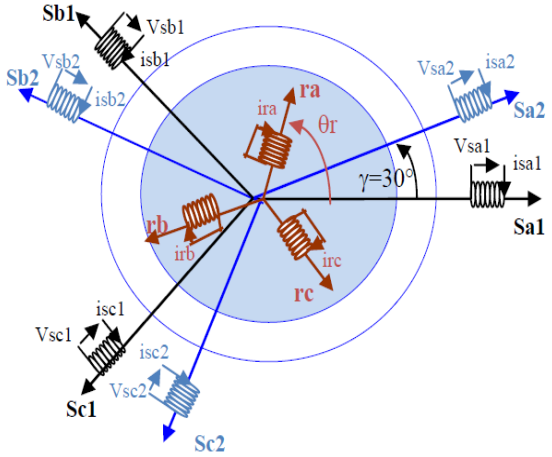

Figure 1. Schematic representation of motor windings of the dual stator induction motor (DSIM).

III. Field Oriented Control of a DSIM

The objective of the vector control of DSIM is to obtain a decoupled control of the electromagnetic torque and the rotor flux as in DC machines [17, 22, 35].

The Indirect Field-Oriented-Control (IFOC) is the most commonly used because of its relative simplicity and low implementation cost. The indirect rotor field oriented control (IRFOC) [17, 31] consists of annulling the quadrature component of the rotor flux $\varphi_{qr} = 0$. Consequently, the reference flux is $\varphi_r^* = \varphi_{dr}$.

By applying this principle into Eqs. (1), (2), (3) and (4), with $\omega_g = \omega_s - \omega_r$, we obtained:

$$\begin{aligned}
T_e &= p \frac{L_m}{L_m + L_r} \varphi_r^* \left(i_{qs1} + i_{qs2}\right) \\
0 &= R_r i_{qr} + \omega_g \varphi_r^* \\
i_{qr} \left(L_r + L_m\right) &= L_m \left(i_{qs1} + i_{qs2}\right)
\end{aligned} \tag{5a}$$

$$\begin{aligned}
\varphi_r^* &= L_m \left(i_{ds1} + i_{ds2}\right) \\
\frac{\mathrm{d}}{\mathrm{d}t} \varphi_r^* &= 0
\end{aligned} \tag{5b}$$

By replacing Eqs. (5) into Eqs. (2), the stator flux equations become:

$$\begin{aligned}
\varphi_{ds1,2} &= L_{s1,2} i_{ds1,2} + \varphi_r^* \\
\varphi_{qs1,2} &= L_{s1,2} i_{qs1,2} + T_r \varphi_r^* \omega_g
\end{aligned} \tag{6}$$

with $T_r = L_r / R_r$

By replacing Eqs. (6) in Eqs. (1), the following voltages equations can be expressed by:

$$\begin{aligned}
V_{ds1,2} &= R_{s1,2} i_{ds1,2} + L_{s1,2} \frac{\mathrm{d} i_{ds1,2}}{\mathrm{d}t} - \\
&\quad - \omega_s \left(L_{s1,2} i_{qs1,2} + T_r \varphi_r^* \omega_g\right) \\
V_{qs1,2} &= R_{s1,2} i_{qs1,2} + L_{s1,2} \frac{\mathrm{d} i_{qs1,2}}{\mathrm{d}t} + \\
&\quad + \omega_s \left(L_{s1,2} i_{ds1,2} + \varphi_r^*\right)
\end{aligned} \tag{7}$$

According to this model, we notice that the voltage equations V_{ds1}, V_{qs1}, V_{ds2}, V_{qs2} influence the current system i_{ds1}, i_{qs1}, i_{ds2}, i_{qs2}, the flux $\varphi_r^* = \varphi_{dr}$ and the torque T_e

For decoupling the axes d and q, we define a new set of four command variables: V_{ds1a}, V_{qs1a}, V_{ds2a}, V_{qs2a} :

$$\begin{aligned}
V_{ds1,2} &= V_{ds1,2a} - e_{ds1,2} \\
V_{qs1,2} &= V_{qs1,2a} - e_{qs1,2}
\end{aligned} \tag{8}$$

The terms of compensation that must be added are:

$$\begin{aligned}
e_{ds1,2} &= \omega_s \left(L_{s1,2} i_{qs1,2} + T_r \varphi_r^* \omega_g\right) \\
e_{qs1,2} &= \omega_s \left(L_{s1,2} i_{ds1,2} + \varphi_r^*\right)
\end{aligned} \tag{9}$$

Fig. 2 shows the reconstitution of voltages $V_{ds1,2}$, $V_{qs1,2}$.

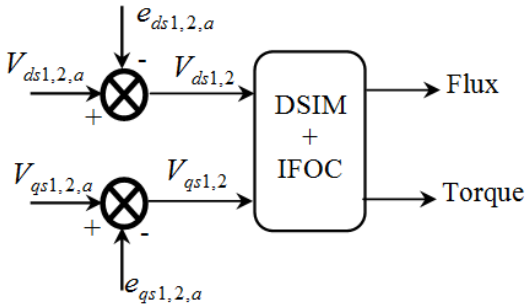

Figure 2. Reconstitution of voltages $V_{ds1,2}$ and $V_{qs1,2}$.

Thus, Eqs. (7) are replaced by:

$$\begin{aligned}
V_{ds1,2a} &= R_{s1,2} i_{ds1,2} + L_{s1,2} \frac{\mathrm{d} i_{ds1,2}}{\mathrm{d}t} \\
V_{qs1,2a} &= R_{s1,2} i_{qs1,2} + L_{s1,2} \frac{\mathrm{d} i_{qs1,2}}{\mathrm{d}t}
\end{aligned} \tag{10}$$

Hence, the actions on the d and q axes are completely decoupled. The decoupling procedure may be observed in Fig. 3. For the adjustment of the speed of the DSIM, starting from the reference speed and the real speed, the fuzzy controller (FC) provides the torque reference T_{ref}. The bloc of Field Weakening generats the reference flux φ_r^*. The indirect field oriented control (FOC) principle is used to

generate the corresponding reference voltages $V_{ds1,\ 2}$ and $V_{qs1,\ 2.}$ A Park reverse transformation (*dq-abc*) calculates the stator reference voltages. These voltages are used to fix the control of each PWM inverter.

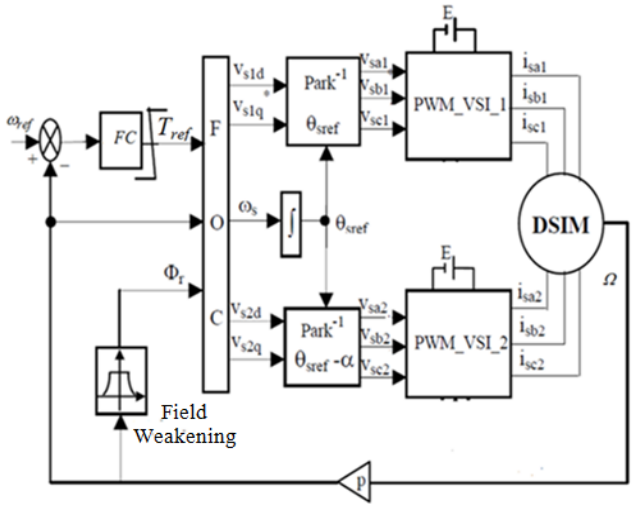

Figure 3. The decoupling procedure of the actions on the *d* and *q* axes.

IV. PI Fuzzy Control

We consider a nonlinear system whose dynamic control equation is described in the following iterative form:

$$T_{ref}(t) = T_{ref}(t-1) + K_{dce}\ \Delta T_{nref}(t) \tag{11}$$

where $\Delta T_{nref}(t)$ is the error variation and K_{dce} is an adapting coefficient.

A. Fuzzification

The error between the reference signal and the process signal acts directly on the control (the gains of the fuzzy regulator are recalculated in real time as a function of this error). The speed, error denoted $e(t)$ is defined by:

$$e(t) = \omega_{ref} - \omega_r(t) \tag{12}$$

The derivative of the speed error is approximated by:

$$\frac{\mathrm{d}e(t)}{\mathrm{d}t} \cong \frac{e(t+1)-e(t)}{T_s} \tag{13}$$

where T_s is the sampling period.

The error and the derivative of the error are given respectively by:

$$e(t) = K_e\ e_n(t)$$
$$\frac{\mathrm{d}e(t)}{\mathrm{d}t} = K_{de}\ \frac{\mathrm{d}e_n(t)}{\mathrm{d}t} \tag{14}$$

where K_e and K_{de} are two adaptation coefficients.

B. Inference table

Once the fuzzy presentation stage has been completed, the gains estimated by the adaptation mechanism using the Lyapunov theory are sent to the fuzzy controller to construct the output $T_{ref}(t)$. The fuzzy rules take the following forms [14, 27]: **NB** - Negative Big; **NS** - Negative Small; **EZ**: Equal Zero; **PS** - Positive Small; **PB** - Positive Big. Considering the variation of the fuzzy sets associated with the control, the inference rule matrix is given in Table 1.

TABLE I. INFERENCE RULES

ΔT_{nref}		e_n				
		NB	**NM**	**EZ**	**PM**	**PG**
$\dot{e}_n(t)$	**NB**	NB	NB	NS	NS	EZ
	NS	NB	NS	NS	EZ	PS
	EZ	NS	NS	EZ	PS	PS
	PS	NS	EZ	PS	PS	PB
	PB	EZ	PS	PS	PB	PB

C. Defuzzification

For the defuzzification, the center-of-gravity method described in [13] was used:

$$\Delta T_{nref}(t) = \frac{\sum_{j=1}^{25} \mu_{A1j} e_n(t)\ \mu_{A2j} \frac{\mathrm{d}e_n}{\mathrm{d}t}\ C_j\ S_j}{\sum_{j=1}^{25} \mu_{A1j} e_n(t)\ \mu_{A2j} \frac{\mathrm{d}e_n}{\mathrm{d}t}\ S_{jj}} \tag{15}$$

where the following notations have been used:

S_j - the function surface of belonging the decision of the rule;

C_j - the gravity center of the function of belonging to the rule decision;

j - the current number of the fuzzy rule.

D. Structure of the proposed adaptive fuzzy controller

In order to minimize the instantaneous error between the actual speed and the reference speed, the gains K_e, K_{dce} are recalculated in real-time by applying a Lyapunov adaptation algorithm. Fig. 4 illustrates schematically the principle of the proposed adaptive fuzzy control.

E. Determining the gains of PI-fuzzy controller

The mechanical equation of the DSIM is expressed in the following form:

$$\frac{J}{p}\frac{\mathrm{d}}{\mathrm{d}t}\omega_r(t) = C_e - C_r - \frac{f_r}{p}\omega_r(t) \tag{16}$$

Eq. (16) can be rewritten in the form below:

$$\frac{\mathrm{d}}{\mathrm{d}t}\omega_r(t) = -a_p\ \omega_r(t) + b_p\ T_e(t) - d_p\ T_r \tag{17}$$

where a_p, b_p, d_p are constants of the DSIM.

On the adaptive fuzzy control based on the Lyapunov stability theory, the control is matched by the electromagnetic torque:

$$T_e(t) = T_{ref}(t) = T_{ref}(t-1) + K_{dce}\ \Delta T_{nref}(t). \tag{18}$$

By replacing (18) in (17), we obtain the following equation form:

$$\frac{\mathrm{d}}{\mathrm{d}t}\omega_r(t) = -a_p\omega_r(t) + b_p T_{ref}(t-1) + b_p K_{dce}\Delta T_{nref}(t) - d_p T_r. \tag{19}$$

The error and its derivative are used to construct the basis of the adaptation mechanism of the adaptive fuzzy controller. They are given by:

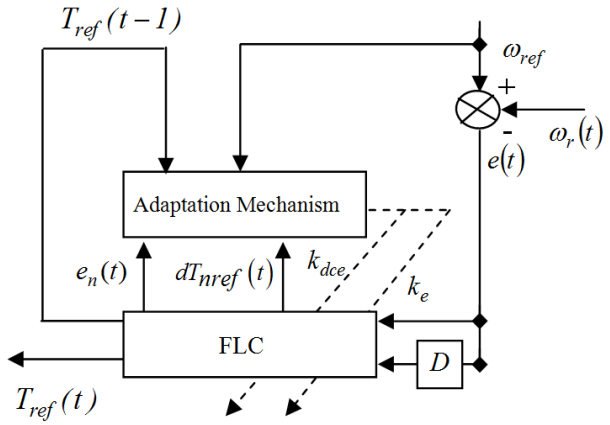

Figure 4. Structure of the proposed adaptive fuzzy control.

$$e(t)=\omega_{ref}-\omega_r(t);$$
$$\frac{\mathrm{d}}{\mathrm{d}t}e(t)=\frac{\mathrm{d}}{\mathrm{d}t}\omega_{ref}-\frac{\mathrm{d}}{\mathrm{d}t}\omega_r(t). \quad (20)$$

Since, $\omega_{ref}=const.$, $\frac{\mathrm{d}}{\mathrm{d}t}\omega_{ref}=0$, and the derivative of the speed error becomes:

$$\frac{\mathrm{d}}{\mathrm{d}t}e(t)=-\frac{\mathrm{d}}{\mathrm{d}t}\omega_r(t) \quad (21)$$

F. Analysis of the stability

We consider the Lyapunov function:

$$F=\frac{1}{2}(e^2+\frac{1}{\gamma_1}k_e^2+\frac{1}{\gamma_2}k_{dce}^2) \quad (22)$$

The time derivative of the Lyapunov function is:

$$\frac{\mathrm{d}F}{\mathrm{d}t}=e\frac{\mathrm{d}e}{\mathrm{d}t}+\frac{k_e}{\gamma_1}\frac{\mathrm{d}k_e}{\mathrm{d}t}+\frac{k_{dce}}{\gamma_2}\frac{\mathrm{d}k_{dce}}{\mathrm{d}t} \quad (23)$$

Bt replacing, the expression of time derivative of the Lyapunov function becomes:

$$\frac{\mathrm{d}F}{\mathrm{d}t}=-a_pK_e^2e_n^2+\frac{K_e}{\gamma_1}\left(\gamma_1e_nA+\frac{\mathrm{d}K_e}{\mathrm{d}t}\right)$$
$$-\frac{K_{dce}}{\gamma_2}\left(\gamma_2b_pK_ee_nd\,T_{nref}(t)-\frac{\mathrm{d}K_{dcee}}{\mathrm{d}t}\right) \quad (24)$$

with:

$$A=\left|\left(a_p\omega_{ref}-b_pT_{ref}(t-1)\right)\right| \quad (25)$$

The gains of a fuzzy regulator must be defined considering the only necessary and sufficient condition of Lyapunov stability:

$$\frac{\mathrm{d}F}{\mathrm{d}t}<0 \quad (26)$$

The inequality is verified by imposing the following adaptation conditions:

$$K_e=-\int\gamma_1e_nA\,\mathrm{d}t \quad (27)$$

$$K_{dce}=\int\gamma_2b_pK_ee_ndC_{nref}(t)\,\mathrm{d}t \quad (28)$$

where γ_1 and γ_2 are positive constants.

Finally, we obtain:

$$\frac{\mathrm{d}F}{\mathrm{d}t}=-a_pK_e^2e_n^2 \quad (29)$$

The Lyapunov function will determine the gains of the PI-fuzzy controller to ensure the convergence of the actual speed of the DSIM to its reference value.

The parameters of the Lyapunov function are chosen to ensure an always negative derivative of the Lyapunov function.

For the adjustment of the speed of the DSIM by the adaptive fuzzy controller based on the Lyapunov theory (AFLC), the method presented in Fig. 4 is applied.

V. Simulation Results

In order to show the feasibility of the proposed AFLC, simulation studies of the drive system based on the DSIM were carried out using MATLAB/Simulink.

The nominal values of the parameters used in the simulations are listed in the Appendix.

The parameters of the proposed AFLC are selected as γ_1 and γ_2 and have the values 0.56 and 6, respectively. Therefore, the initial values of the gains k_e and k_{dce} are 15.5 and 6.2, respectively.

To illustrate the effectiveness of the proposed controller, the closed-loop system is examined under four scenarios, i.e., the step change of load torque, the speed reversal, the variation of the inertia coefficient and the robustness against parameter uncertainties.

The block diagram of the investigated field oriented control for a voltage source inverter fed DSIM is presented in Fig. 5.

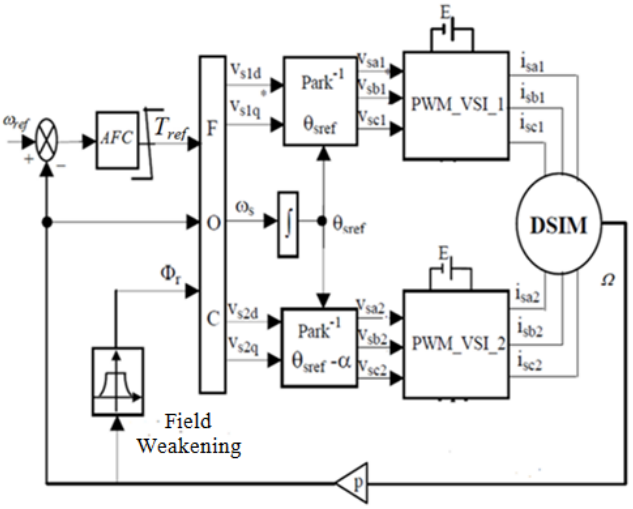

Figure 5. Control of the DSIM based on the AFLC.

A. System Behaviour by Variation of Load Torque

To investigate the effectiveness of proposed robust control, the performance of the PI-FLC and PI-AFLC are compared (Figs. 6, 7).

This test concerns the speed evolution and the disturbance rejection of the two controllers when the DSIM is operated at 100 rad/s under no load and a load torque variation 14 Nm is suddenly applied at then moment t=1 s and removed at the moment t=2 s, respectively.

Fig. 7 shows that the PI-AFLC gives good performances, rejects the load disturbance very rapidly.

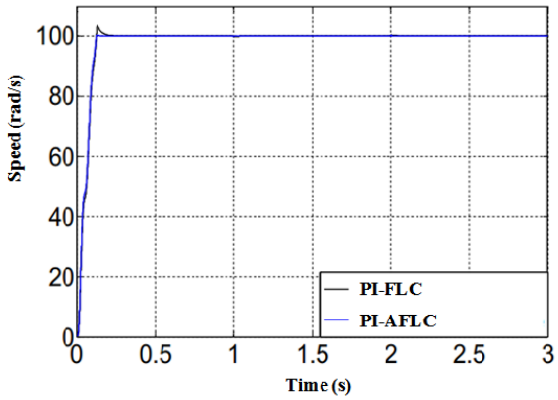

Figure 6. Dynamic response of the speed.

In contrast, the PI fuzzy controller significantly deviated from the reference speed value with an overshoot.

Fig. 8 shows the electromagnetic torque. The AFLC algorithm reacts faster than the PI-fuzzy controller when load torque is suddenly applied and removed.

Fig. 9 shows the evolution of the PI-AFLC gains K_{dce}, K_e.

The adaptive gains change automatically to compensate the variation in the speed, hence driving the motor speed to the desired response even though the motor plant dynamics have changed.

The gains increases gradually until the command speed is reached. After that, the gains are kept constant.

B. System Behaviour by Speed Reversal

At the moment t=1.5 s, the motor reference speed is changed from +100 rad/s to -100 rad/s. The performance of the proposed PI-AFLC for such kind of speed reverse is shown in Figs. 10-12, respectively, which present plots of the actual speed, electromagnetic torque and adaptive gains.

It can be observed that the adaptive gains change automatically to compensate the speed variation.

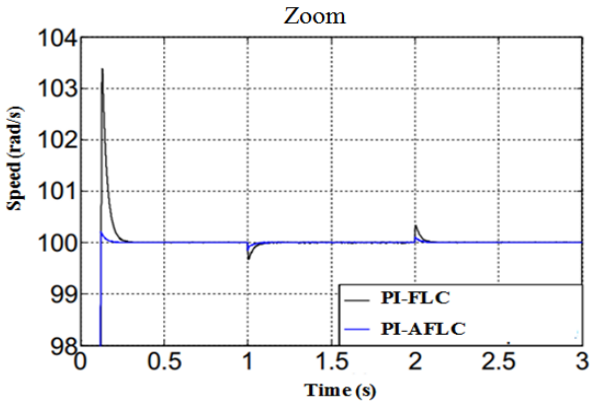

Figure 7. Zoom of the speed response.

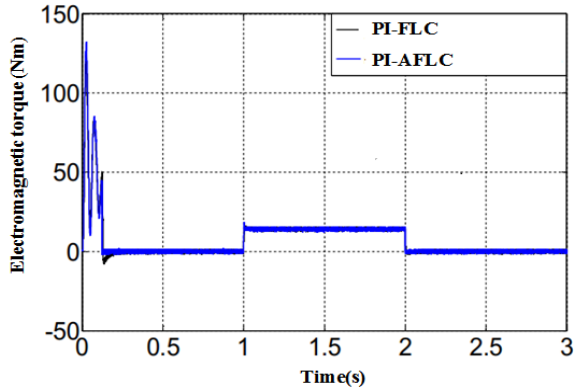

Figure 8. The electromagnetic torque variation.

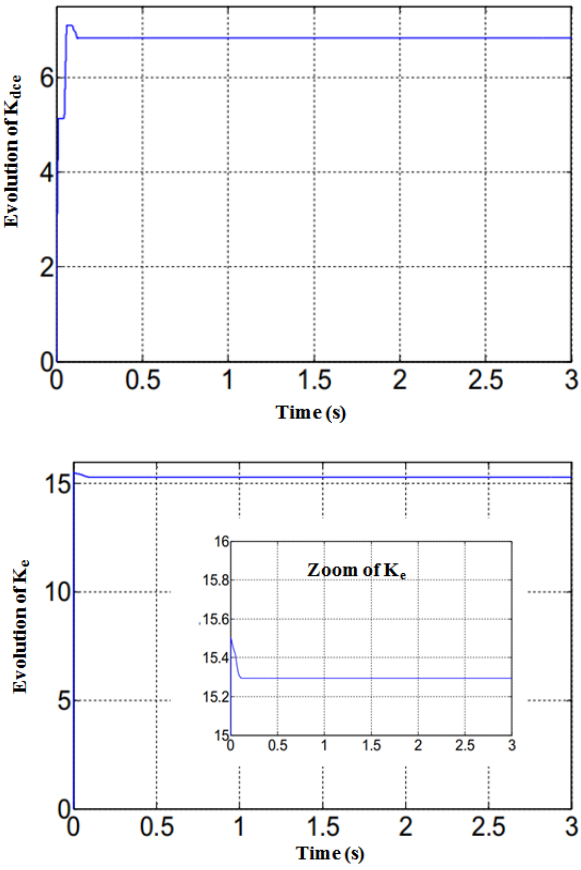

Figure 9. Evolution of the AFLC gains K_{dce} and K_e.

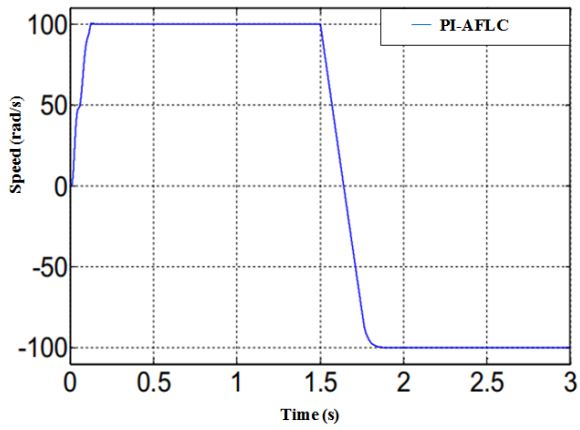

Figure 10. Speed response.

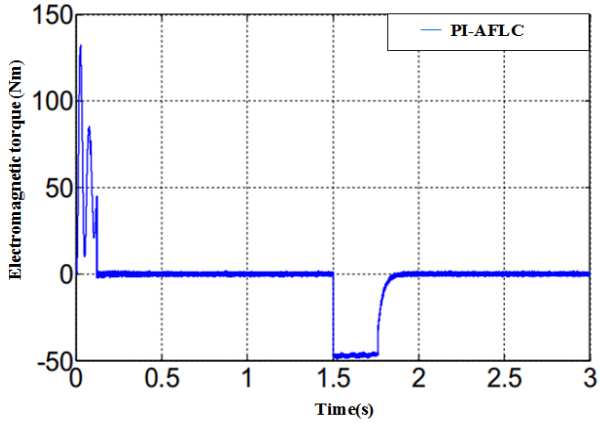

Figure 11. The electromagnetic torque.

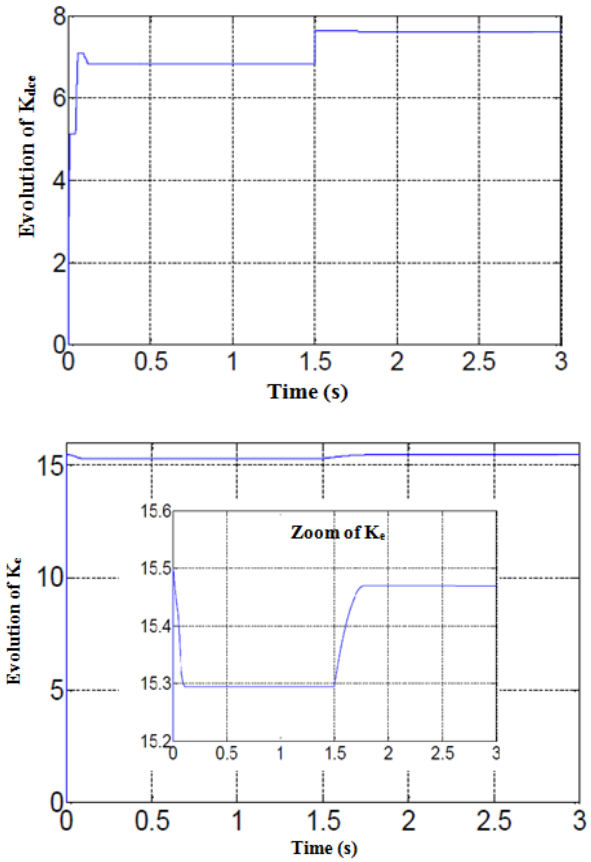

Figure 12. Evolution of the AFLC gains K_{dce}, K_e.

C. *System Behaviour by Variation of the Inertia*

Figs. 13-15 show the drive dynamic under different values of the inertia with a constant reference speed equal to 100 rad/s by using the PI-FLC controller and PI-AFLC controller. The speed tracking is significantly enhanced by using the improved schemes, when the inertia *J* increases by 150% and decreases by 50%, respectively.

D. *System Behaviour by Variation of the Rotor Resistance*

The rotor resistance is sensitive to the temperature which changes gradually with respect to the load and the ambient temperature. In order to test the influence of DSIM parameter variations on the performances of the proposed PI-AFLC, the rotor resistance parameter sensitivity is tested for the two scenarios for increases by 150% and decreases by 50%.

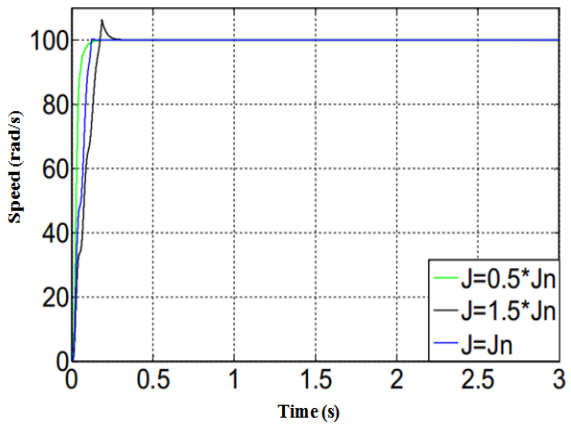

Figure 13. Simulation results for inertia coefficient variation

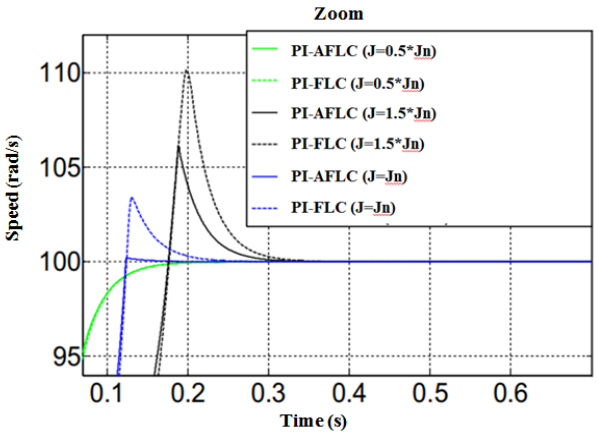

Figure 14. Zoom of the speed response.

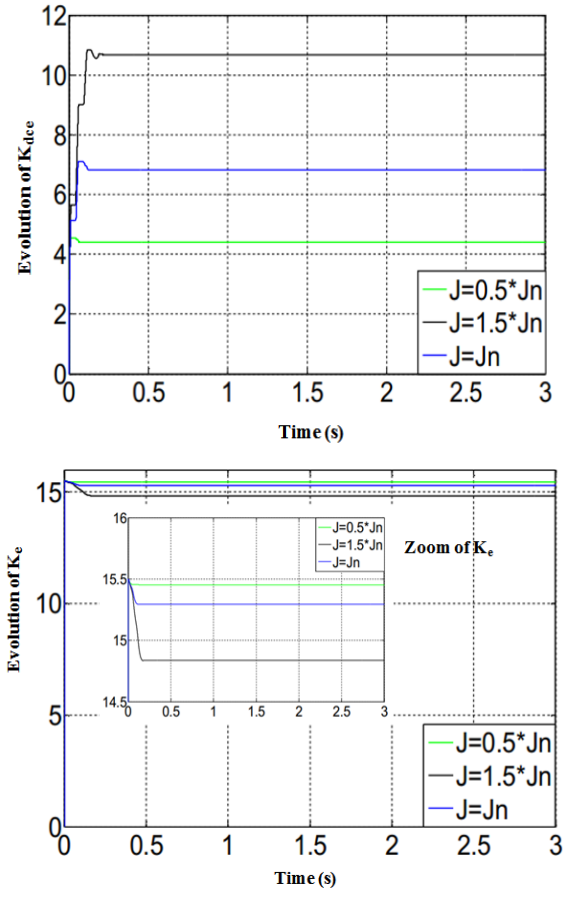

Figure 15. Evolution of the AFLC gains K_{dce}, K_e.

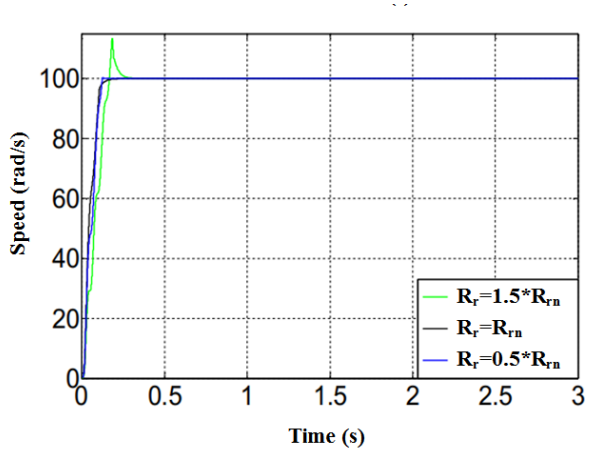

Figure 16. Simulated results for rotor resistance variation.

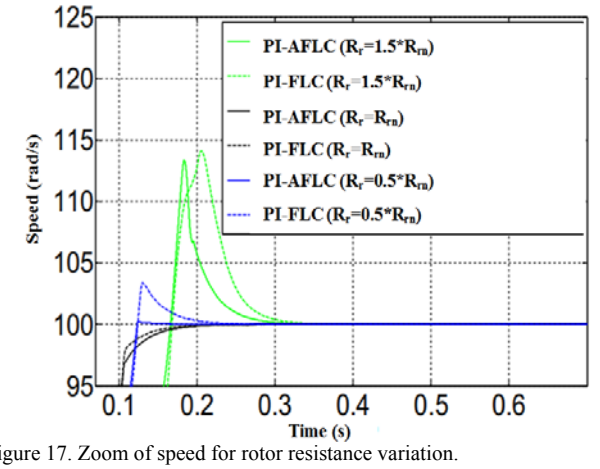

Figure 17. Zoom of speed for rotor resistance variation.

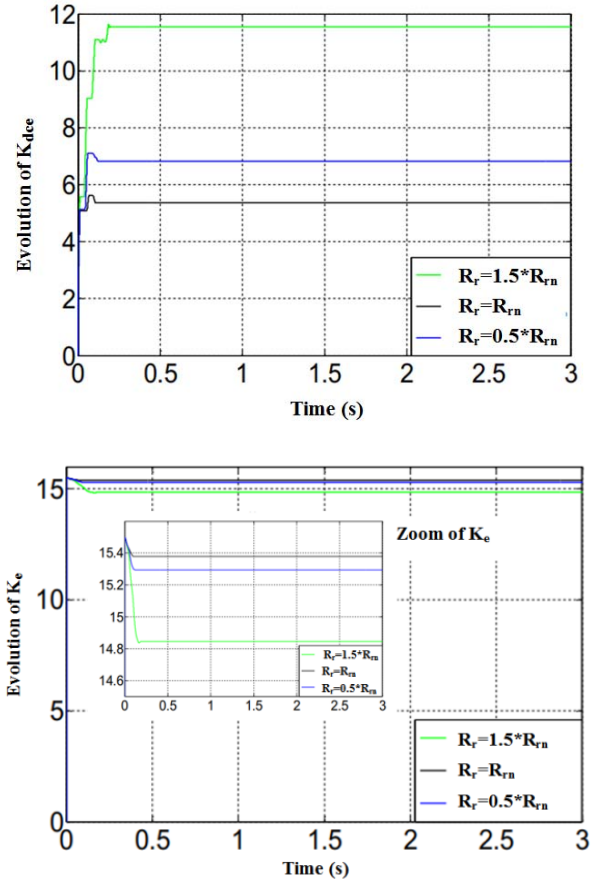

Figure 18. Evolution of the AFLC gains $K_{dce,}$ and K_e.

The actual speed, the zoom of speed and the adaptive gains are shown in Figs. 16-18; it can be observed that PI-FLC schemes have a considerable error due to R_r variation. However remarkable improvements are achieved by the adaptive fuzzy control approach

VI. Conclusion

In this paper, a comparative study between the fuzzy control and the adaptive fuzzy control has been presented for speed controller of the DSIM. The proposed AFLC method does not require any parameters or experimental information on the variation of PI-fuzzy regulator gains.

The stability theory-based adaptation system is used to approximate the gains Ke and Kdce for assuring the stability of the control in real time

The proposed controller offers significant tracking performance and robustness against parameters variations compared to the conventional PI-fuzzy controller. Using the proposed algorithm, any variation in the motor dynamics will not affect the controller performance. Consequently, this algorithm is suitable for applications requiring a high tracking accuracy when external disturbances occur.

Appendix

DSIM parameters used for simulation

Rated power P	5 kW
Stator resistance R_{s1}= R_{s2}	3.72 Ω
Rotor resistance R_r	2.12 Ω
Stator inductance L_s	0.022 H
Rotor inductance L_r	0.006 H
Mutual inductance L_m	0.3672 H
Number of pole pairs p	1
Inertia J	0.0662 kg m2
Viscous friction coefficient f_r	0.001 kg m2/s

REFERENCES

[1] Y. Zhao, T. A. Lipo, "Space vector PWM control of dual three-phase induction machine using vector space decomposition," IEEE Trans. on industry applications, 31(5), 1995 pp. 1100–1109, doi:10.1109/28.464525.

[2] D. Hadiouche, H. Razik, A. Rezoug, "On the modeling and design of dual-stator windings to minimize circulating harmonic currents for VSI fed AC machines," IEEE Trans. on Industry Applications, vol. 40, no. 2, pp. 506–515, 2004, doi:10.1109/TIA.2004.824511.

[3] H. Kouki, M.B. Fredj, H, Rehaoulia, "Vector space decomposition for double star induction machine modeling," 2014 15th International Conference on Sciences and Techniques of Automatic Control and Computer Engineering (STA), pp. 581-586, 2014, doi:10.1109/STA.2014.7086691.

[4] O. Ojo, Z. Wu, "Speed Control of a Dual Stator Winding Induction Machine," APEC 07 - Twenty-Second Annual IEEE Applied Power Electronics Conference and Exposition, pp.: 229 – 235, 2007, doi:10.1109/APEX.2007.357519.

[5] Z. Oudjebour, E.M. Berkouk, M.O. Mahmoudi, "Stabilization by New control technique of the input DC voltages of five-level diode - Clamped inverters. Application to double star induction machine," 2012 2nd International Symposium on Environment Friendly Energies and Applications, pp. 541 - 544 2012, doi:10.1109/EFEA.2012.6294034.

[6] H. Kouki, M.B. Fredj, H. Rehaoulia, "Modeling of double star induction machine including magnetic saturation and skin effect," 10th International Multi-Conferences on Systems, Signals & Devices 2013 (SSD13), pp. 1–5, 2013, doi:10.1109/SSD.2013.6564045.

[7] M. F. Minouni, R. Dhifaoui, "Speed identification for deadbeat rotor flux level control of double-star induction machine," IEEE International Conference on Systems, Man and Cybernetics, Vol. 5(4), pp. , 2002, doi:10.1109/ICSMC.2002.1176322.

[8] H. Hammache, D. Moussaoui, K. Marouani, T. Hamdouche, "Magnetic properties in double star induction machine," 2008 18th

International Conference on Electrical Machines, pp. 1 – 6, 2008, doi:10.1109/ ICELMACH.2008.4799961.

[9] K. Pienkowski, "Analysis and Control of Dual Stator Winding Induction Motor, Archives of Electrical Engineering," Ed. Polish Academy of Sciences, Vol. 61, Nr. 3, pp. 421-438, 2012, doi:10.2478/v10171-012-0033-z.

[10] H. Khouidmi, A. Massoun, A. Meroufel, "Dual Star Induction Motor Drive Modelling – Supplying and Control," International Journal of Electrical Power Engineering, Vol. 5, pp. 28-34, 2011, doi:10.3923/ ijepe.2011.28.34.

[11] L. A. Mier Quiroga, J.S. Benitez Read, R. Lopez Callejas, J. A. Segovia de los Rios; R. Pena Eguiluz; F. J. Jimenez Ramirez, "Adaptive Fuzzy Control System for a Squirrel Cage Induction Motor," IEEE Latin America Transactions, vol. 15, pp. 795– 805, 2017 doi:10.1109/TLA.2017.7910191.

[12] H. Amimeur, D. Aouzellag, R. Abdessemed, K. Ghedamsi, "Sliding mode control of a dual-stator induction generator for wind energy conversion systems," International Journal of Electrical Power and Energy Systems, vol. 42, pp. 60–70, 2012, doi:10.1016/j.ijepes.2012.03.024.

[13] S. Meroufel, A. Massoum, A. Bentaallah, P. Wira, "Double star induction motor direct torque control with fuzzy sliding mode speed controller," Rev. Roum. Sci. Techn. Electrotechn. et Energ. vol. 62, pp. 31–35, 2017, http://revue.elth.pub.ro/viewpdf.php?id=641.

[14] T. Laamayad, F. Naceri, R. Abdessemed and S. Belkacem, "A Fuzzy Sliding Mode Strategy for control of the Dual Star Induction Machine," Journal of Electrical Engineering, Romania, Vol. 13, No.3, pp. 216-223, 2013, http://www.jee.ro/covers/art.php?issue=WH13418Z6520W4ffacce834 0e7.

[15] Z. Tir, Om.P. Malikb, A.M. Eltamaly, "Fuzzy logic based speed control of indirect field oriented controlled Double Star Induction Motors connected in parallel to a single six-phase inverter," Electric Power Systems Research, Elsevier, vol. 134, pp. 126–133, 2016, doi:10.1016/j.epsr.2016.01.013.

[16] K. Kouzi, T. Seghier and A. Natouri, "Fuzzy Speed Sensorless Vector Control of Dual Star induction Motor Drive using MRAS Approach," International Journal of Electronics and Electrical Engineering IJEEE, Vol. 3, No. 6, pp. 445-450, December 2015, http://www.ijeee.net/ uploadfile/2015/0710/20150710050309220.pdf.

[17] S. Lekhchine, T. Bahi, Y. Soufi, "Indirect rotor field oriented control based on fuzzy logic controlled double star induction machine," International Journal of Electrical Power and Energy Systems, Elsevier, vol. 57, pp. 206–211, 2014 .

[18] T. H. Liu, and M.T. Lin, "A Fuzzy Sliding Mode Controller, Design for a Synchronous Reluctance Motor Drive," IEEE. Trans. AES-32(2), pp. 1065-1076, 1996, doi:10.1109/7.532265.

[19] H. Khouidmi, H. Benbouali, "Reduced-Order Sliding Mode Observer-based Speed Sensorless Vector Control of Double Stator Induction Motor," Acta Polytechnica Hungarica, Vol. 11, No. 6, 2014.

[20] U. S. Lu and J. S. Chen, "A self-organizing fuzzy sliding controller design for a class of nonlinear servo system," IEEE Trans. IE-41, pp. 492-502, 1994, doi:10.1109/41.315267.

[21] E. Merabet, H. Amimeur, F. Hamoudi, R. Abdessemed, "Self-Tuning Fuzzy Logic Controller for a Dual Star Induction Machine," Journal of Electrical Engineering and Technology, Korea, Vol. 6, No. 1, pp.133-138, 2011, http://home.jeet.or.kr/archives/view_articles.asp?seq=39.

[22] N. Farah, M.H.N. Talib, Z. Ibrahim, M. Azri, Z. Rasin, "Self-Tuned Output Scaling Factor of Fuzzy Logic Speed Control of Induction Motor Drive," 7th IEEE International Conference on System Engineering and Technology (ICSET), pp. 134-139 2017, doi:10.1109/ICSEngT. 2017. 8123434.

[23] K. Zeb, Z. Ali, K. Saleem, W. Uddin, M. A. Javed, N. Christofides, "Indirect field-oriented control of induction motor drive based on adaptive fuzzy logic controller," Electrical Engineering, (Archiv für Elektrotechnik), Springer, vol. 99, pp. 803–815, 2017, doi:10.1007/s00202-016-0447-5.

[24] J. Ch. Lo, Y.H. Kuo, "Decoupled Fuzzy Sliding Mode Control," IEEE Trans. on Fuzzy Systems, Vol. 6, No. 3, pp. 426-435, 1998, doi:10.1109/91.705510.

[25] H. Mohammed, A. Meroufel, "Contribution to the Neural network speed estimator for sensor-less fuzzy direct control of torque application using double stars induction machine," 2014 International Conference on Electrical Sciences and Technologies in Maghreb (CISTEM), pp. 1-8, 2014, doi:10.1109/CISTEM.2014.7077064.

[26] L. A. Zadeh, Fuzzy sets, "Information and Control," Elsevier, vol. 8(3), pp. 338–353, 1965, doi:10.1016/S0019-9958(65)90241-X.

[27] E. H. Mamdani, "Application of fuzzy algorithms for control of simple dynamic plant," Proc. IEEE, Vol.121, No.12, pp.1585–1588, 1974, doi:10.1049/piee.1974.0328.

[28] F. Hamidia; A. Abbadi; M. S. Boucherit, "Direct torque controlled dual star induction motors (in open and closed loop)," 2015 4th International Conference on Electrical Engineering (ICEE), pp. 1 – 6, 2015, doi:10.1109/INTEE.2015.7416772.

[29] H. B. Hamed, M.D. Mehdi, S. Lassaad, "Direct rotor field-oriented control of a dual star induction machine," 2017 International Conference on Green Energy Conversion Systems (GECS). doi:10.1109/GECS.2017.8066234.

[30] I. Kortas, A. Sakly, M. F. Mimouni, "Optimal vector control to a double-star induction motor," Energy, vol. 131, Issue C, pp. 279-288, 2017. doi:10.1016/j.energy.2017.03.058

[31] M. H. Lazreg, A. Bentaallah, "Speed sensorless vector control of double star induction machine using reduced order observer and MRAS estimator," 2017 6th International Conference on Electrical Engineering (ICEE), doi:10.1109/ICEE-B.2017.8192150.

[32] R. Sadouni and A. Maroufel, "Performances Comparative Study of Field Oriented Control (FOC) and Direct Torque Control (DTC) of Dual Three Phase Induction Motor," International Journal of Circuits, Systems and Signal Processing, Vol. 6, No. 2, pp. 163-170, 2012, http://naun.org/main/NAUN/circuitssystemssignal/16-079.pdf.

[33] B. Tabbache, S. Douida, M. Benbouzid, D. Diallo, A. Kheloui, "Direct torque control of five-leg inverter-dual induction motor powertrain for electric vehicles," Electrical Engineering vol. 99, No. 3, pp. 1073–1085, 2017, doi:10.1007/s00202-016-0467-1.

[34] A. Azib, D. Ziane, T. Rekioua, A. Tounzi, "Robustness of the direct torque control of double star induction motor in fault condition," Rev. Roum. Sci.Techn. Électrotechn. et Énergn 61(2), pp. 147–152, 2016, http://revue.elth.pub.ro/index.php?action=details&id=573.

[35] M. Bouziane, M. Abdelkader, "A Neural Network Based Speed Control of a Dual Star Induction Motor," International Journal of Electrical and Computer Engineering (IJECE), Vol. 4, No. 6, pp. 952-961, 2014, doi:10.11591/ijece.v4i6.6343.